INTERNATIONAL JOURNAL FOR NUMERICAL METHODS IN FLUIDS, VOL. 15, 1037–1057 (1992)

AUTOMATIC MESH GENERATION METHOD FOR SHALLOW WATER FLOW ANALYSIS

KAZUO KASHIYAMA

Department of Civil Engineering, Chuo University, 1-13-27 Kasuga, Bunkyo-ku, Tokyo 112, Japan

AND

TSUYOSHI OKADA

Scientific and Technical Service Sales Department, Japan Information Processing Service, 2-4-24 Toyo, Koto-ku, Tokyo 135, Japan

SUMMARY

This paper presents a new automatic mesh generation method for the finite element analysis of shallow water flow. The key feature of this method is that the finite element mesh can be generated so that the element Courant number is nearly constant in the whole domain. It follows that the numerical stability and accuracy improve automatically. Moreover, the finite element mesh data, including the data of water depth, can be prepared automatically. The three-node triangular element is used for the finite element. In order to show the efficiency of the method presented, the mesh obtained by this method is applied to some shallow water flow analyses. This method is shown to be a useful and powerful tool for the preparation of optimal finite element mesh data for shallow water flow analysis.

KEY WORDS Automatic mesh generation method Courant number Numerical accuracy and stability Shallow water flow Tsunami wave propagation

INTRODUCTION

Numerical simulation is becoming a useful and powerful tool to study shallow water flow with the advangate of computer hardware and software. A number of numerical methods based on the finite element method have been presented to analyse shallow water flow,[1] since the finite element method can easily treat arbitrary boundaries and variable water depth. These numerical methods are usefully applied at the stage of planning and design of various coastal and offshore structures. However, if the configurations of the boundary and water depth are complicated, the following problems arise. First of all, it is indicated that the appropriate partition of elements must be realized in accordance with the variation of wavelength in order to get satisfactory numerical accuracy. The following empirical rule is usefully applied: the element size should be everywhere less than 10% of the wavelength.[2] Since the wavelength varies according to water depth, it is difficult to generate a finite element mesh which satisfies this requirement in a domain with complex geometry. Secondly, preparing finite element mesh data in the case of large-scale computations is time-consuming. In order to overcome this problem, a number of automatic mesh generation methods have been developed in recent years. However, most of these methods are not developed for shallow water analysis, which requires the data of water depth, but for

0271–2091/92/211037–21$15.50

Received October 1991
Revised March 1992

structural analysis. Therefore the data of water depth are usually entered after the preparation of the plane mesh data. The input data of water depth is really important for not only numerical accuracy but also numerical stability. Thacker,[3] Westwood and Holtz[4] and Nielsen and Skovgaard[5,6] developed automatic mesh generation methods for shallow water analysis; however, these conventional methods have not introduced the concept of numerical stability and accuracy.

This paper presents a new automatic mesh generation method for the finite element analysis of shallow water flow. The key feature of this method is that the finite element mesh data can be generated so that the element Courant number is nearly constant in the whole domain with complex geometry. From this, the appropriate partition of elements is realized in accordance with the variation of water depth. It follows that the numerical stability and accuracy will improve automatically. Moreover, the finite element mesh data, including the data of water depth, can be prepared automatically. The three-node triangular element is used in this paper. In order to show the efficiency of this method, it has been applied to some shallow water flow analyses such as tsunami wave propagation.

AUTOMATIC MESH GENERATION METHOD

Basic concept

The Courant number can be defined as

$$C = U\,\Delta t/\Delta x, \tag{1}$$

where C denotes the Courant number, U is the velocity, Δt is the time increment of numerical integration in time and Δx is the element size. The velocity U is assumed to be the sum of the phase velocity U_w and the current velocity U_c:

$$U = U_w + U_c. \tag{2}$$

Since the value of current velocity U_c is unknown and small compared with the value of phase velocity U_w, the Courant number can be written as

$$C = U_w\,\Delta t/\Delta x. \tag{3}$$

Assuming the long-wave theory, the velocity U_w can be expressed as

$$U_w = \sqrt{(gh)}, \tag{4}$$

where g is the gravitational acceleration and h is the water depth. The present method generates the finite element mesh data so that the element Courant number is nearly constant in the whole domain:

$$C = U\,\Delta t/\Delta x = \text{constant}. \tag{5}$$

Introducing equation (4) into equation (5), the following equivalent condition can be easily obtained:

$$L/\Delta x = \text{constant}, \tag{6}$$

where L denotes the wavelength. Therefore it is possible to generate the finite element mesh in accordance with the variation of wavelength using this concept.

Algorithm

The present mesh generation method is a sort of node distribution method;[7,8] namely, the nodes on the boundary of the analytical region are entered first and the interior nodes are

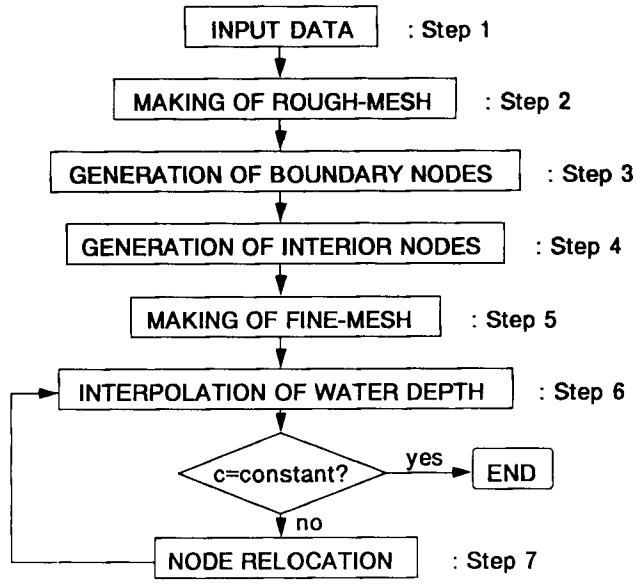

Figure 1. Flow chart

generated subsequently to make the finite element mesh. Two types of mesh are used in this paper. One of them is referred to as the rough mesh, which is used for the interpolation of element size function and water depth. The other is the fine mesh, which is used for the finite element analysis. Figure 1 shows the flow chart of this method.

The algorithm of this method is as follows.

Step 1. The nodes and their co-ordinates are entered along the geometrical boundary and at the points where the water depth is known using a chart and digitizer.
Step 2. The rough mesh is prepared using the nodes given in Step 1.
Step 3. The new nodes on the boundary are generated so that the element Courant number is nearly constant.
Step 4. The new nodes in the analytical region are generated so that the element Courant number is nearly constant in the whole domain.
Step 5. The fine mesh is prepared using the nodes given in Steps 1, 3 and 4.
Step 6. The water depths of the new nodes are interpolated by linear interpolation using the value of water depth of the rough mesh.
Step 7. The nodal points are relocated so that the element Courant number is constant in the whole domain.

The following explains the details of the above steps using the application example for the port of Hiroshima in Japan shown in Figure 2.

Input data

The input data require nodes along the boundary and nodes with known water depth. The values of the x- and y-co-ordinates and the water depth of these nodal points are entered. The nodes on the exterior boundary (the boundary of the analytical region) are entered in coumnter-clockwise order, while the nodes on the interior boundary (the boundary of structures and islands

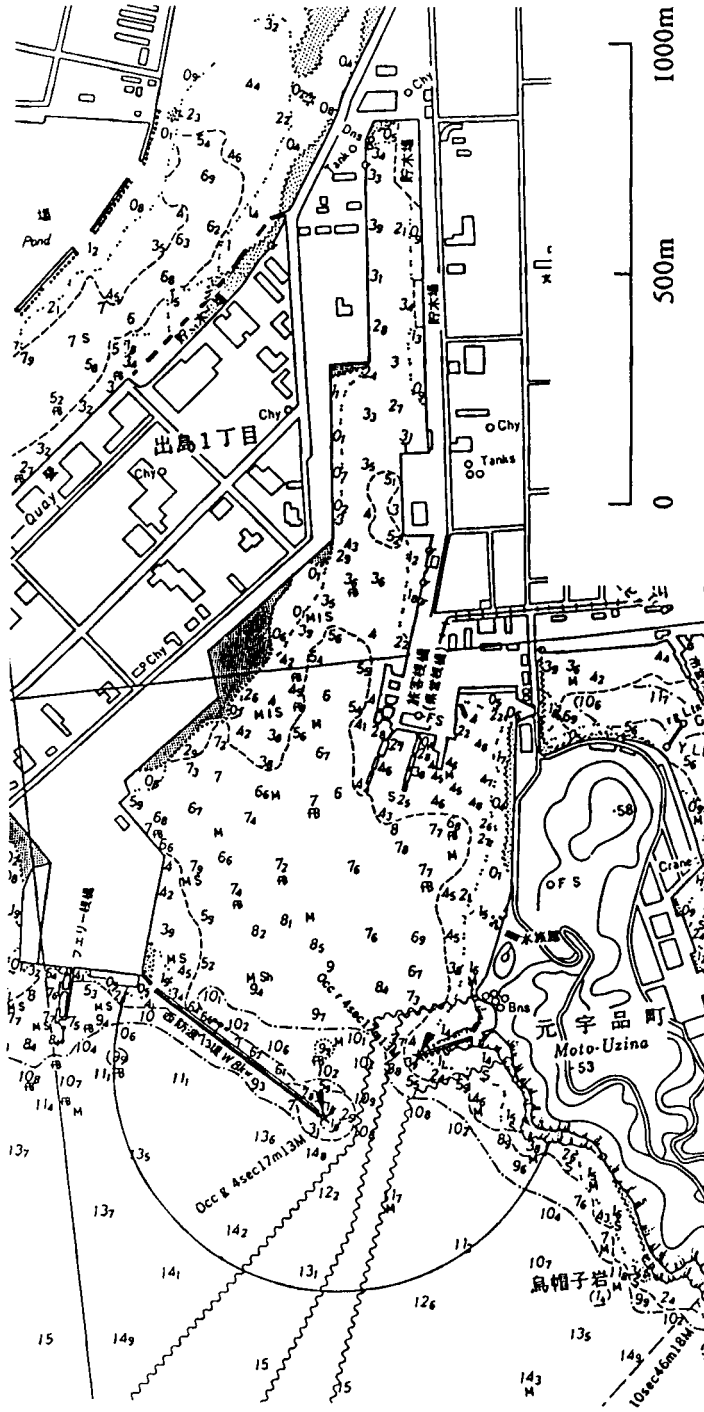

Figure 2. Port of Hiroshima

in the analytical region) are entered in clockwise order. For the remaining input data, the time increment Δt, which is related to the Courant number, and the node interval δ, which is used in the generation of nodes, are entered. In this example the time increment and the node interval are assumed to be 3 s and 1 m respectively. Figure 3 shows the analytical region to be triangulated, in which the dots indicate the nodal points entered as the input data. The total number of input nodes is 314 in this case.

Forming triangular elements

The method of forming triangular elements is as follows. Denoting the line segment A–B as a generation front and the set of all nodes C as shown in Figure 4, it is necessary to determine the

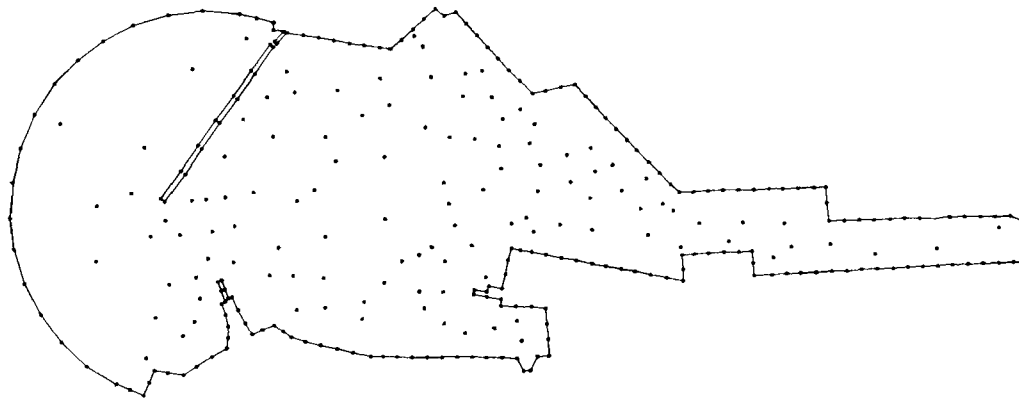

Figure 3. Input data for port of Hiroshima

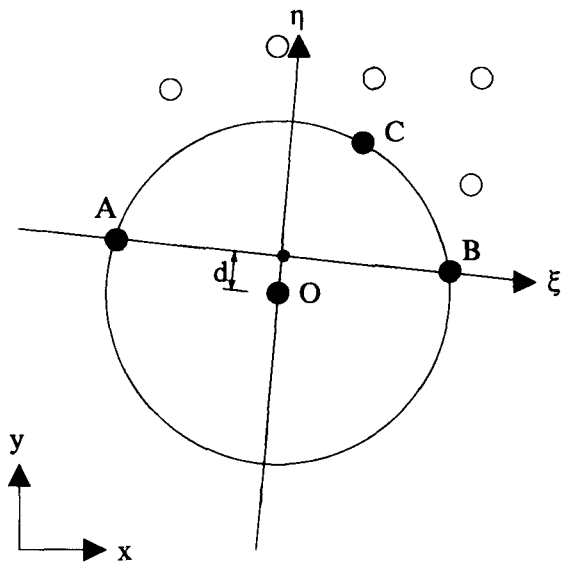

Figure 4. Method of triangulation

node C which forms the triangular element ΔABC with the line segment A–B. To do this, the ξ–η co-ordinate system is introduced. The node C is selected from the nodes which have a positive co-ordinate value of η. After considering the circumcircle of ΔABC centred on the ponit O and establishing the minimum co-ordinate value of O, there is now a sufficient condition to determine the node C. After determination of the node C, the line segment B–C will be a new generation front and the same procedure is repeated. Special treatment is required if one of the nodes of the generation front (A or B) is located on the boundary as shown in Figure 5. In this case the node C is selected from the nodes in the hatched area. Figure 6 shows the finite element idealization of the rough mesh. The total number of elements is 431 in this case. This algorithm is also applied to the triangulation of the fine mesh.

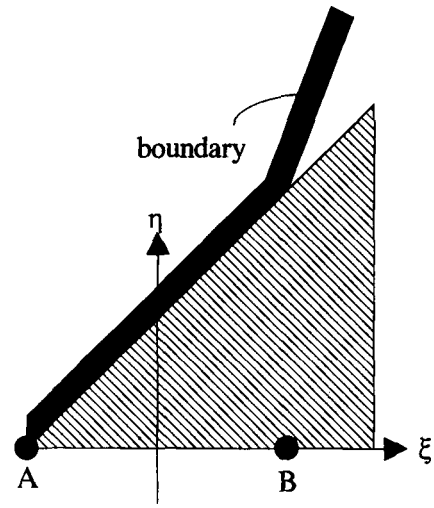

Figure 5. Special consideration

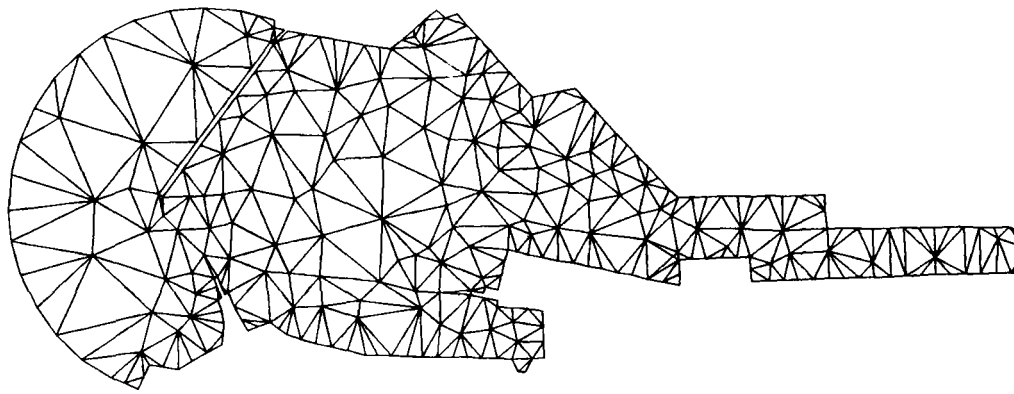

Figure 6. Rough mesh for port of Hiroshima

Generation of boundary nodes

After the preparation of the rough mesh, the new boundary nodes are generated. The generation of nodes can be achieved so that the element Courant number is nearly constant in the whole domain. To do this, a function of element size f, which is referred to as the element size function, can be usefully introduced from equation (1) as

$$f=\Delta x=\Delta t\sqrt{(gh)}, \tag{7}$$

where f represents the element size in the case where the Courant number is 1·0.

Consider a line element (eth element) on the boundary with length L as shown in Figure 7. The element size function at the nodes can be expressed as

$$f_i=\Delta x=\Delta t\sqrt{(gh_i)}, \tag{8}$$

where f_i and h_i denote the element size function and the water depth at the nodes respectively. The generation of new nodes is investigated at intervals δ. The node P can be accepted as a new node in cases where the following equation is satisfied:

$$f_p<l, \tag{9}$$

where f_p is the element size function at node P and l denotes the distance from P to its closest existing node (see Figure 7). Equation (9) can be held when the Courant number is less than 1·0. The value of f_p is given by linear interpolation as

$$f_p=\Phi_1 f_1+\Phi_2 f_2, \tag{10}$$

where f_1 and f_2 are the element size functions at the two ends of the line element and Φ_1 and Φ_2 are the respective linear interpolation functions. In Figure 7 the black square represents the existing interior nodes which satisfy equation (9), while the white squares represent the boundary nodes.

If the new nodes are generated on the curved boundary, it is necessary to fit the new nodes to the boundary. To do this, the Lagrange interpolation method is applied using the nodes of both neighbouring elements. In this example the open boundary of the port is assumed to be a curved boundary.

Generation of interior nodes

The generation of interior nodes is also investigated at intervals δ from the bottom line to the upward direction as shown in Figure 8. Referring to an interior node P, it is necessary to

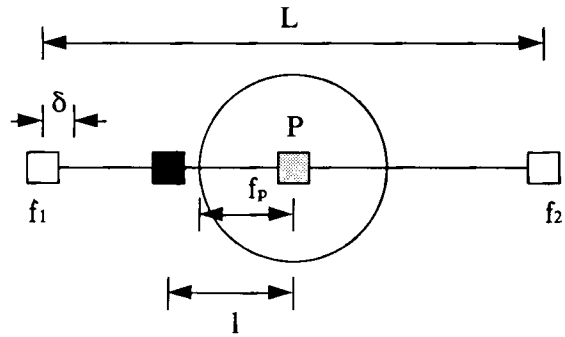

Figure 7. Generation of boundary nodes

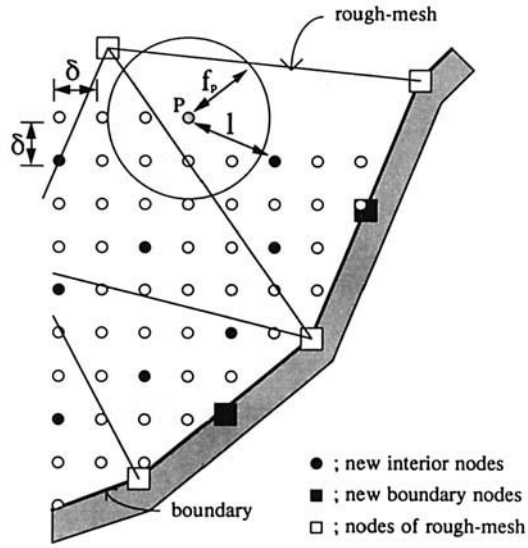

Figure 8. Generation of interior nodes

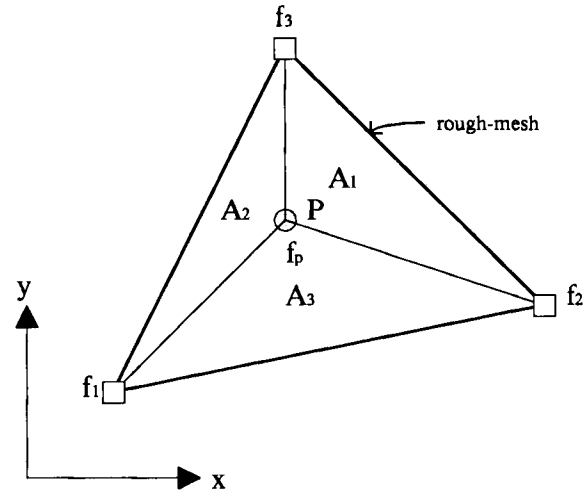

Figure 9. Interpolation of element size function

determine the element of the rough mesh in which the node P is included. To do this, the area co-ordinate is usefully applied.[9] If the node P is included in the triangular element of the rough mesh as shown in Figure 9, the following relation is valid as:

$$A_1 > 0, \qquad A_2 > 0, \qquad A_3 > 0, \tag{11}$$

where A_1, A_2 and A_3 are the areas of the three-node triangles formed by the node P and two of the three vertices of the triangle, in which A_1 can be obtained from

$$A_1 = \tfrac{1}{2}[x_p(y_2 - y_3) + x_2(y_3 - y_p) + x_3(y_p - y_2)]. \tag{12}$$

Having found the element in which the node P is included, the interpolation equation for the element size function can be easily formulated as

$$f_p = \Phi_1 f_1 + \Phi_2 f_2 + \Phi_3 f_3, \tag{13}$$

where f_p is the element size function at node P and f_1, f_2, and f_3 are the element size functions at the three vertices of the triangular element of the rough mesh. The interpolation functions Φ_1, Φ_2 and Φ_3 are based on the linear polynomial.

In case where equation (9) is satisfied, the node P can be accepted as a new interior node (see Figure 8). In Figure 8 the black circles represent the existing interior nodes which satisfy equation (9), while white circles represent the nodes omitted and the squares represent the boundary nodes. Figure 10 shows the distribution of new nodes. It can be seen that the interior nodes are generated in accordance with the variation of water depth. Figure 11 represents the fine finite element idealization using the existing nodes. For triangulation, the method which is used for the rough mesh is also applied. The total numbers of elements and nodes are 6423 and 3489 respectively.

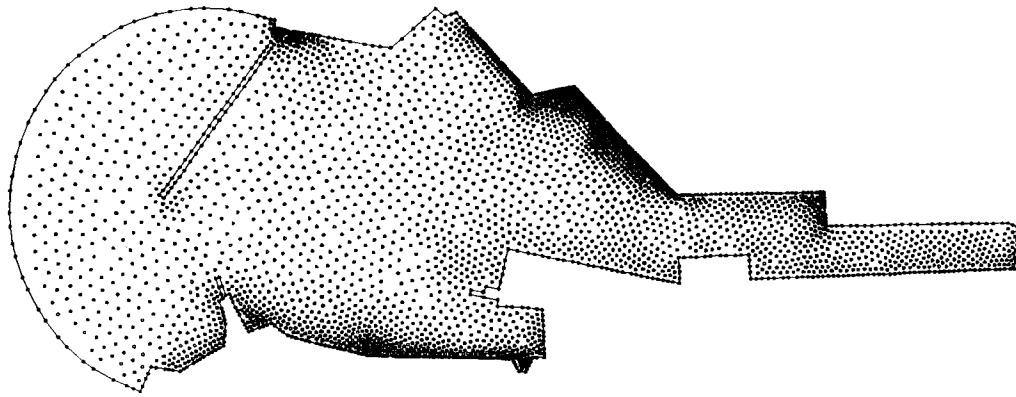

Figure 10. Distribution of nodes

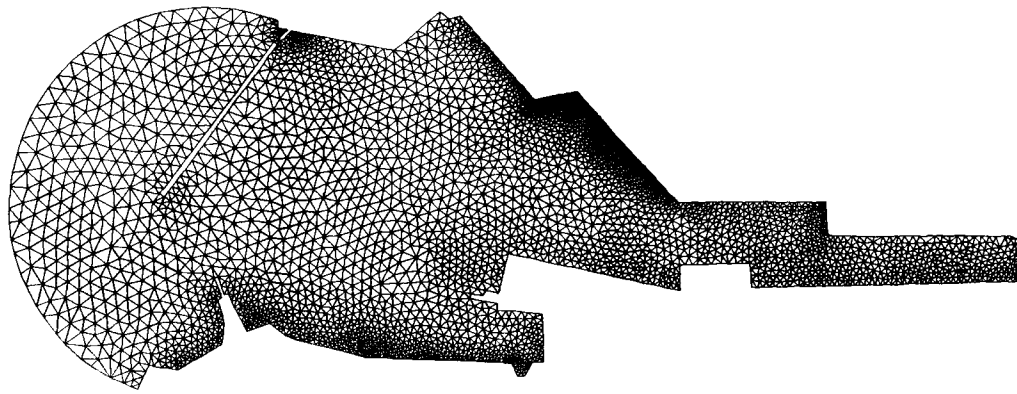

Figure 11. Fine mesh for port of Hiroshima

Interpolation of water depth and node relocation

For the interpolation of water depth, the algorithm used in the interpolation of the element size function is applied. The water depth at node P is interpolated as

$$h_p = \Phi_1 h_1 + \Phi_2 h_2 + \Phi_3 h_3, \tag{14}$$

where h_p is the water depth at node P and h_1, h_2 and h_3 are the water depths at the three vertices of the triangular element of the rough mesh.

The nodal points are relocated using a grid-smoothing scheme[10,11] in order that the element Courant number can be constant in the whole domain and that distortion of the element can be avoided as much as possible. Denoting the new co-ordinate of node P as X_p, the node P is relocated in accordance with (see Figure 12)

$$X_p = \sum_{e=1}^{M_n} C_e A_e X_e \Big/ \sum_{e=1}^{M_n} C_e A_e, \tag{15}$$

where M_n is the total number of elements which share the node P and C_e and X_e are the element Courant number and the co-ordinate of the centroid of the eth element respectively. The hatched area indicates the limit of node relocation for one relocation. Figure 13 shows the finite element

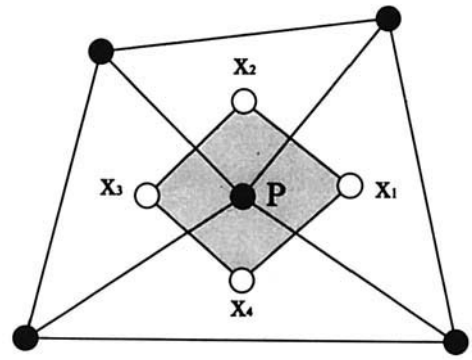

Figure 12. Method of node relocation

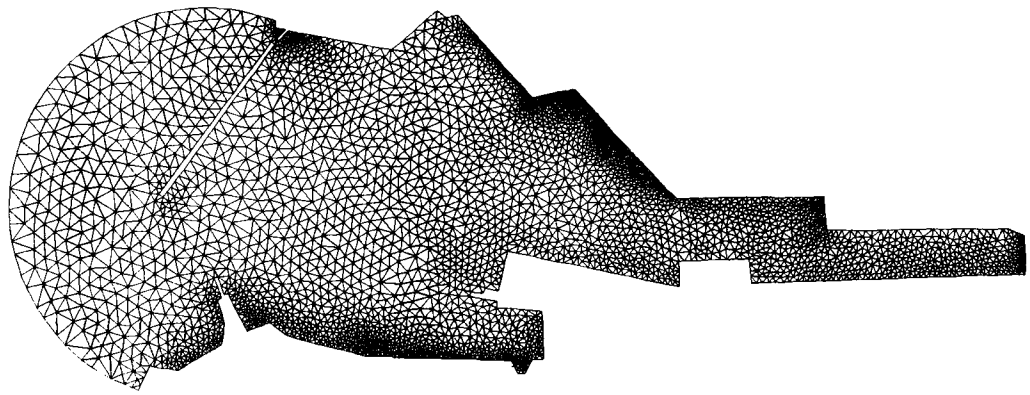

Figure 13. Finite element idealization for port of Hiroshima: $\Delta t = 3$ s, $\delta = 1$ m

idealization after the appliction of node relocation. The node relocation based on equation (15) was applied three times in this paper. The nodes entered as input data are excepted from the application of node relocation. Figure 14 represents the computed water depth diagram. It can be seen that the appropriate partition of elements is realized in accordance with the variation of water depth. Figure 15 represents the distribution of Courant number. In this computation the minimum element length of the traingular element is used for the element length Δx. From this figure it can be seen that more than 80% of the elements fall in the range of 0·7–1·0 and this result can be acceptable for computations. It follows that it is possible to use the time increment as the predictive value of time increment in actual computations.

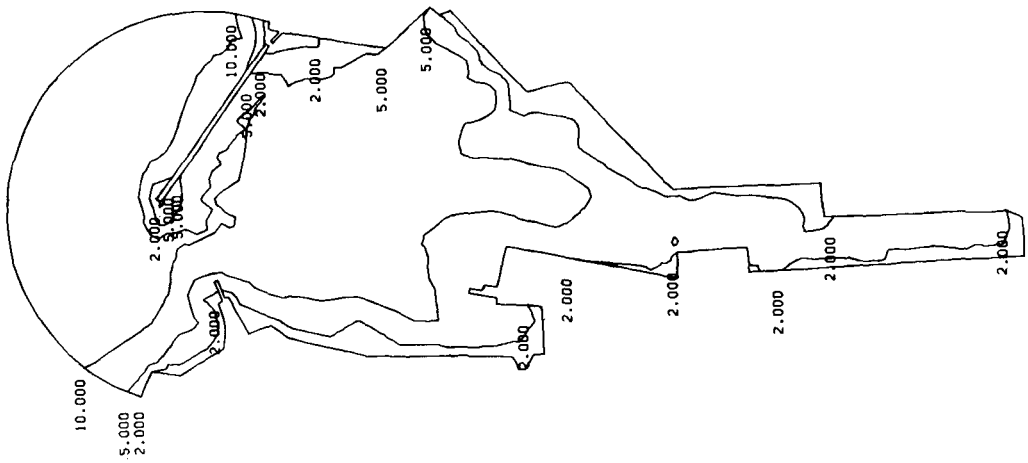

Figure 14. Computed water depth diagram

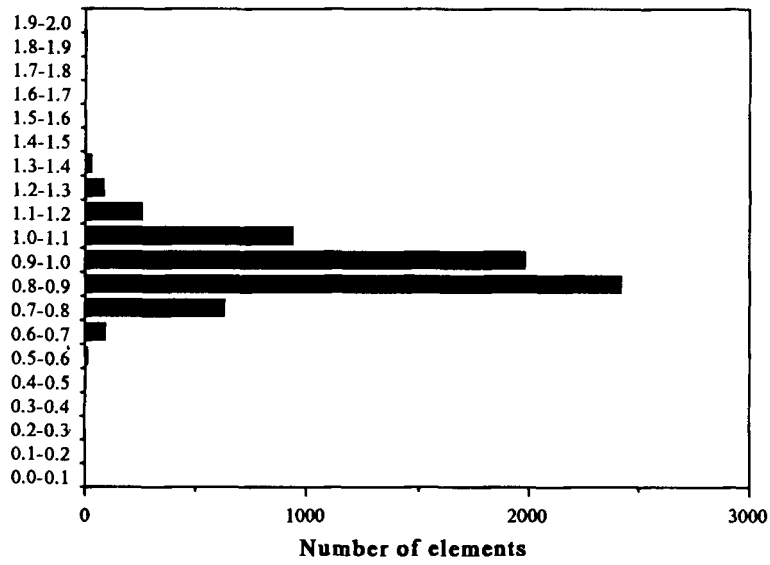

Figure 15. Distribution of element Courant number

The following shows the results using the different input data, the time increment Δt and the node interval δ. Figure 16(a) shows the finite element idealization when Δt and δ are assumed to be 5 s and 5 m respectively. The total numbers of elements and nodes are 1967 and 1129 respectively. Figure 16(b) is the finite element idealization when Δt and δ are assumed to be 4 s and 4 m respectively. In this case the total numbers of elements and nodes are 3105 and 1731 respectively. From these results it is possible to control the total numbers of elements and nodes by choosing the appropriate input data.

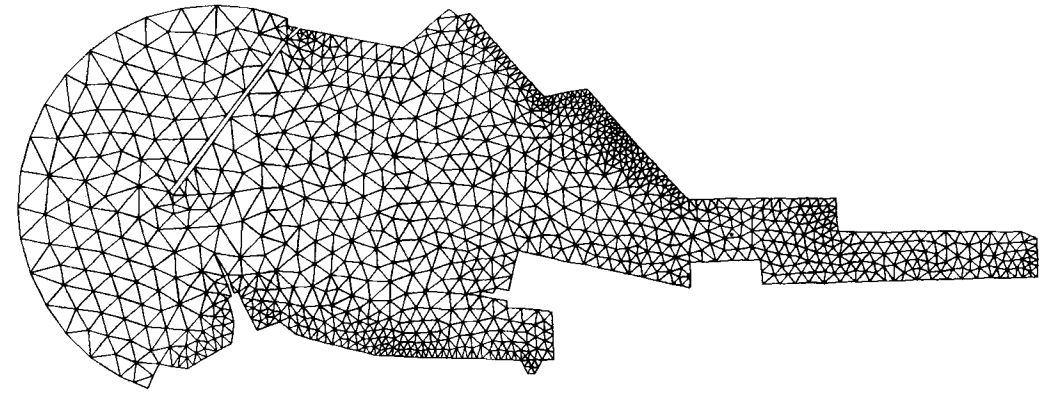

(a)

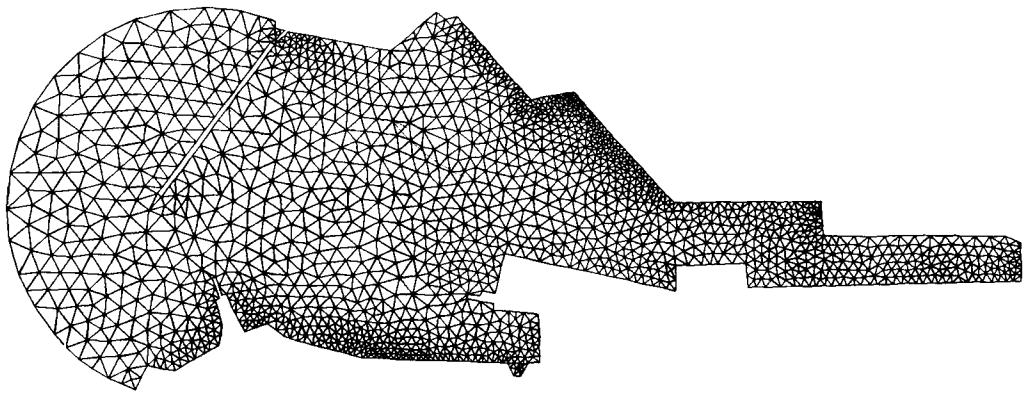

(b)

Figure 16. Finite element idealization: (a) $\Delta t = 5$ s, $\delta = 5$ m; (b) $\Delta t = 4$ s, $\delta = 4$ m

NUMERICAL TEST

In order to show the efficiency of this method, the finite element analysis for the one-dimensional shoaling wave problem with varying water depth is considered in Figure 17. The water depth at the offshore boundary, h_o, is assumed to be 10 m and the bottom slope is assumed to be constant. The computation is performed with the variation of bottom slope. Figure 18 shows the finite element mesh idealizations which are used in this computation. Mesh (a) indicates the finite element mesh with constant element size and mesh (b) is the finite element mesh with constant element Courant number obtained by the present method (Figure 18(b) shows the mesh in the case of $h_0 = 10$ m and $h = 1$ m).

The following shallow water equation is used for the governing equation in this example:

$$\partial u_i / \partial t + u_j u_{i,j} + g\zeta_{,i} = 0, \tag{16}$$

$$\partial \zeta / \partial t + [(h+\zeta)u_i]_{,i} = 0, \tag{17}$$

where u_i is the mean horizontal velocity and ζ is the water elevation. The boundary conditions are expressed in Figure 18.

The selective lumping two-step explicit finite element method[12,13] is applied for the discretization. For the numerical conditions, the incident wave amplitude and wave period are assumed to be 0·5 m and 300 s respectively. The selective lumping parameter is assumed to be 0·93, which is determined by several numerical experiments. Figure 19 shows the comparison of the water

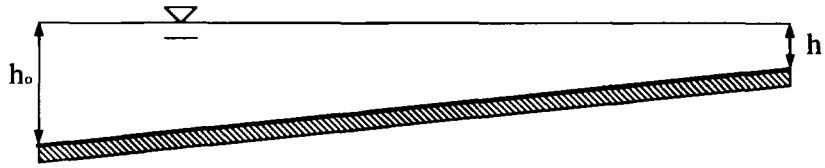

Figure 17. Shoaling wave problem

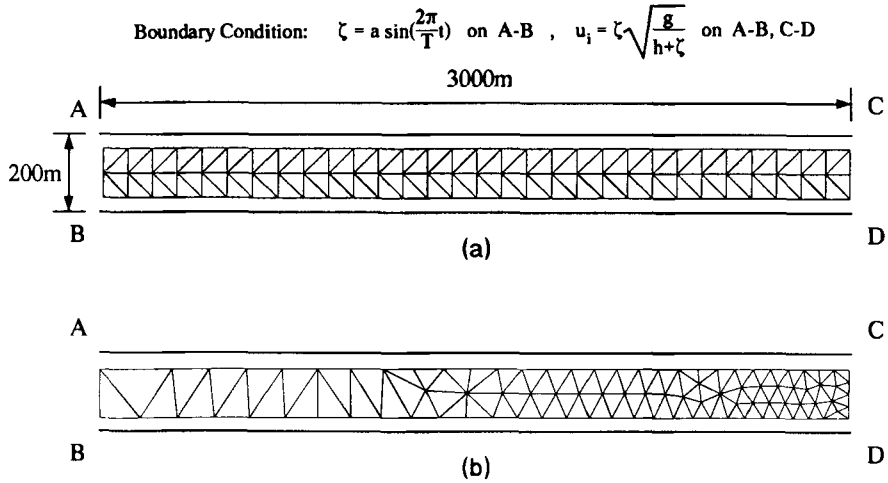

Figure 18. Finite element idealization

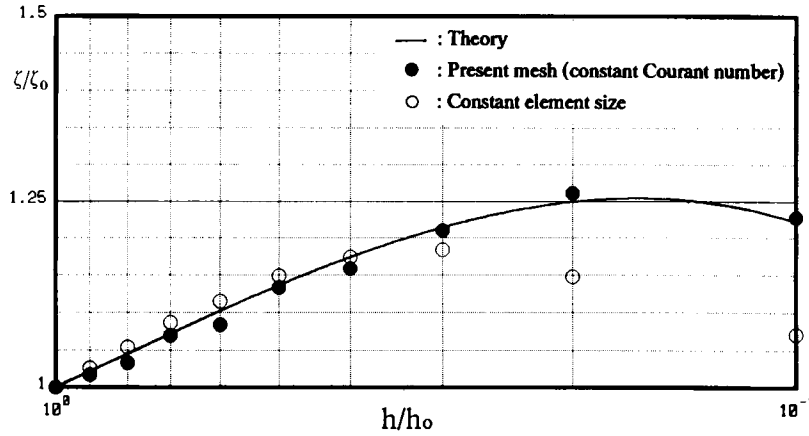

Figure 19. Comparison of water elevation between computed and theoretical results

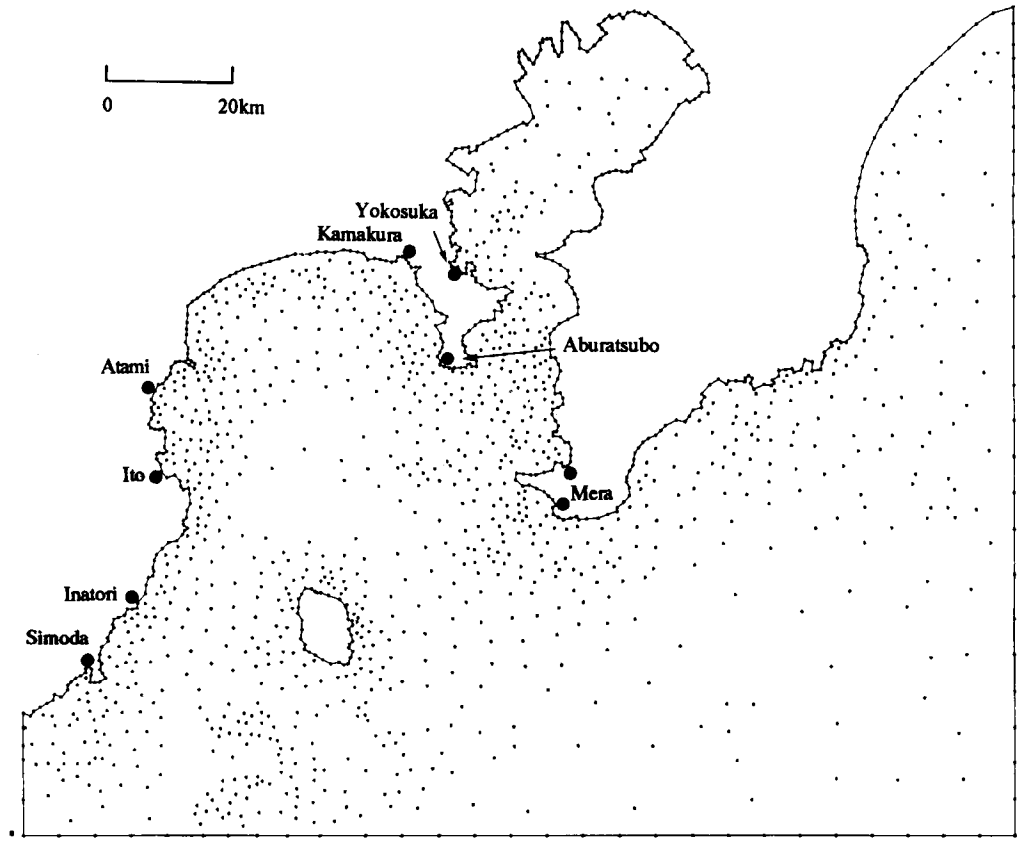

Figure 20. Input data for tsunami wave propagation

elevation between computed results and theoretical results. The abscissa indicates the ratio of water depth and the ordinate indicates the ratio of maximum water elevation, between the value at the offshore boundary A–B and the value at the nearshore boundary C–D, in which the subscripts 'o' express the value at the offshore boundary. In this figure the solid curve represents the theoretical results obtained by Kajiura,[14] the white circles represent the computed results usig mesh (a) with constant element size and the black circles represent the computed results using mesh (b) with constant element Courant number. It can be seen that the computed results using mesh (b) agree with the theoretical results. From this it can be seen that the numerical accuracy can be improved using the mesh obtained by the present method.

TSUNAMI WAVE ANALYSIS

The present method is applied to the analysis of tsunami wave propagation. For the numerical example, the tsunami accompanying the Kanto earthquake of 1923 is chosen. Figure 20 shows the analytical region to be triangulated, in which the dots indicate the nodal points entered as the input data. The total number of input nodes is 1641 in this example. For the other input data, the

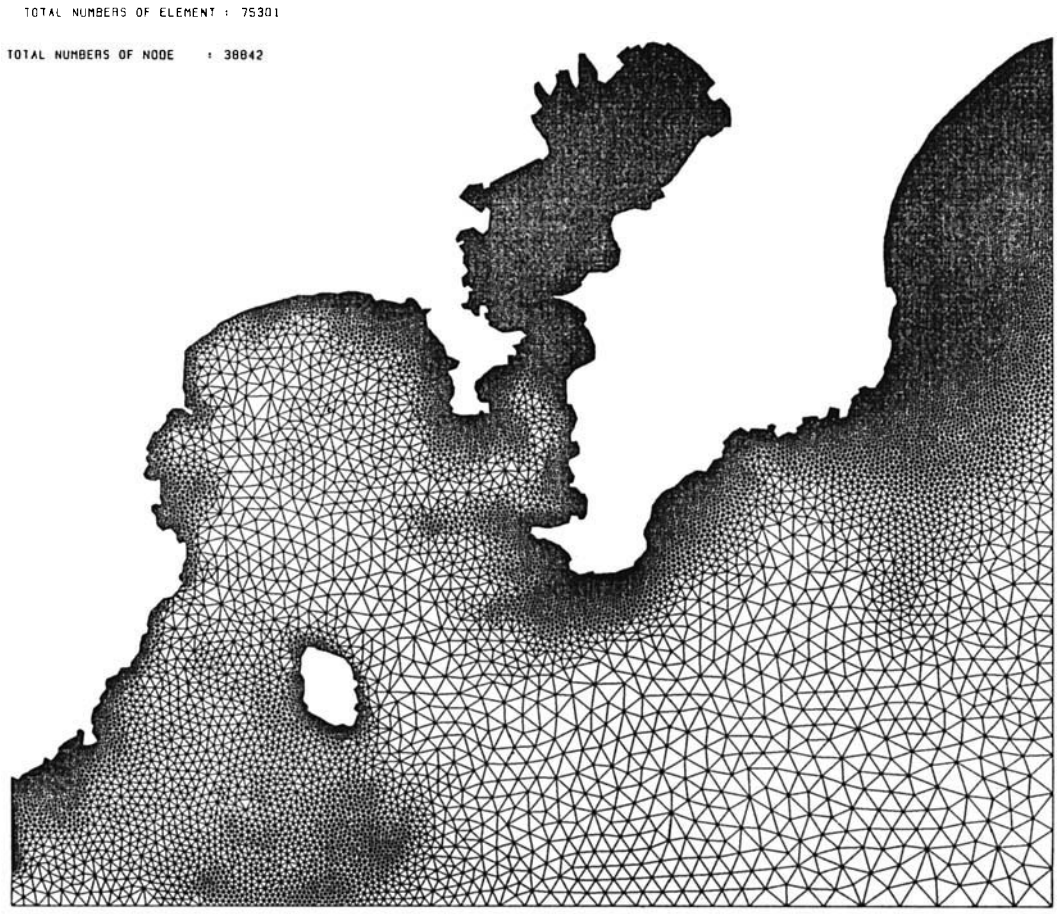

Figure 21. Finite element idealization obtained by the present method

time increment and node interval are assumed to be 20 s and 150 m respectively. The finite element mesh and water depth obtained are shown in Figures 21 and 22 respectively. It can be seen that the appropriate partition of elements is realized in accordance with the variation of water depth. The total numbers of elements and nodes are 75 301 and 38 842 respectively. The computational results are compared with the results obtained by the structured mesh shown in Figure 23, for which the total numbers of elements and nodes are 87 187 and 44 398 respectively. The following linearized shallow water equation including the bottom deformation is used for the governing equation in this example:

$$\partial u_i/\partial t + g\zeta_{,i} = 0, \tag{18}$$

$$\partial(\zeta - b)/\partial t + hu_{i,i} = 0, \tag{19}$$

where b denotes the value of bottom deformation. The computation is started from the state of still water and the bottom deformation which is obtained by surveying is given at the same rate for the first 2 min. Figure 24 shows the distribution of bottom deformation. The $\frac{1}{24}$-values of the surveyed results are used in the computation in accordance with the study of Aida.[15] The selective lumping two-step explicit finite element method is applied for the discretization. For the method

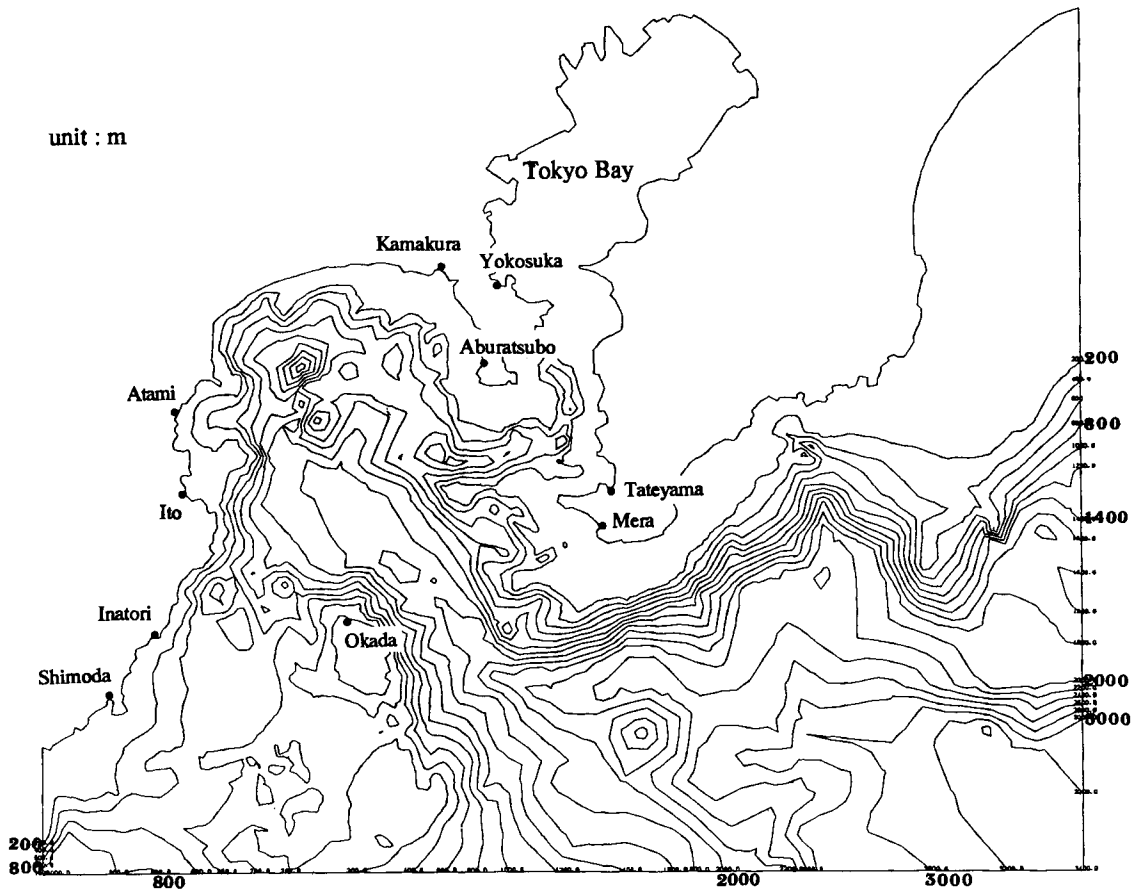

Figure 22. Water depth diagram

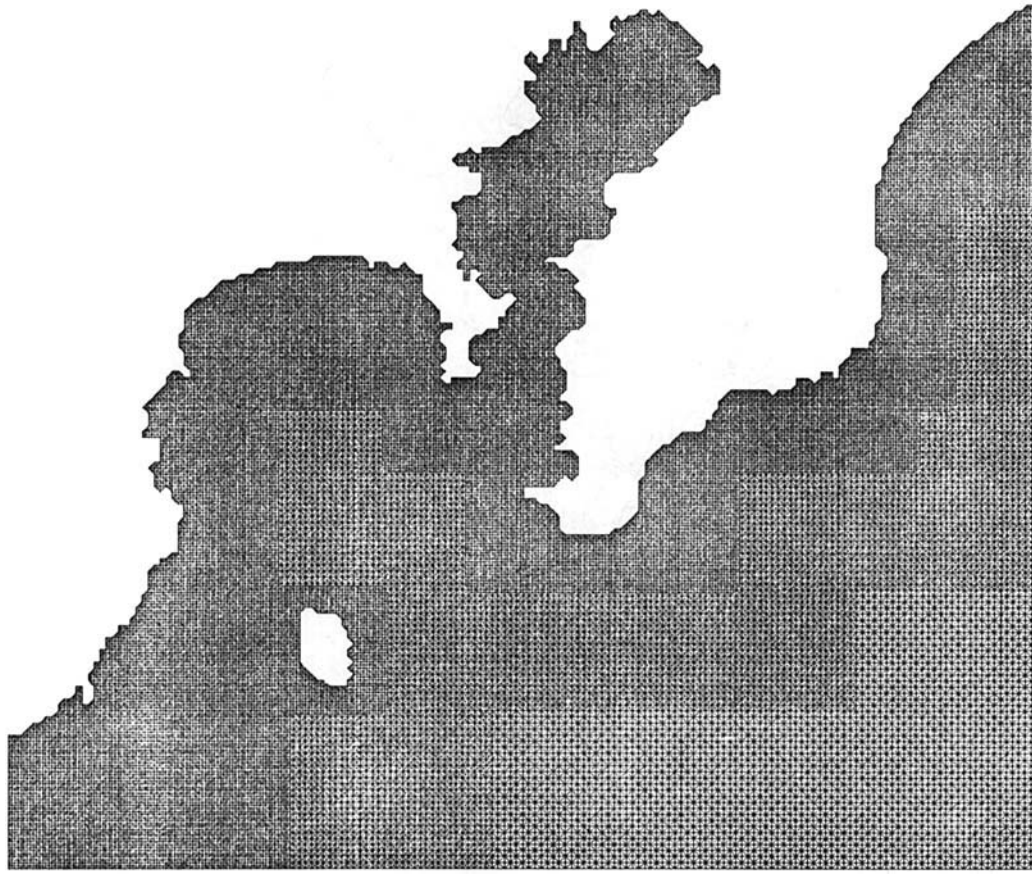

Figure 23. Finite element idealization of structured mesh

of numerical treatment for the open boundary condition, the method presented by Kawahara *et al.*[16] is used in this example. Figure 25 shows a bird's-eye view of the computed tsunami waves 2 and 28 min later. The phenomena of tsunami wave propagation can be clearly seen in these figures. The time history of the computed water elevation at some observation points is shown in Figure 26. In this figure the heavy lines represent the computed results using the mesh obtained by the present method shown in Figure 21 and the fine lines represent the computed results using the structured mesh shown in Figure 23. It can be seen that the computed results using the structured mesh show damping and smoothing phenomena compared with the results using the present mesh. Figure 27 shows the comparison of the maximum water elevation at some observation points. In this figure the black circles represent the observed results, the white circles represent the computed results using the mesh obtained by the present method and the white triangles represent the computed results using the structured mesh. From this figure the computed results using the present mesh agree with the observed results. Moreover, using the present method, it is possible to take a larger value of the time increment, since the element Courant number is nearly constant in the whole domain. The limit of the time increment Δt is 6 s for the present mesh, which is three times larger than the limit for the structured mesh. It follows that the computational time can be reduced using the present mesh.

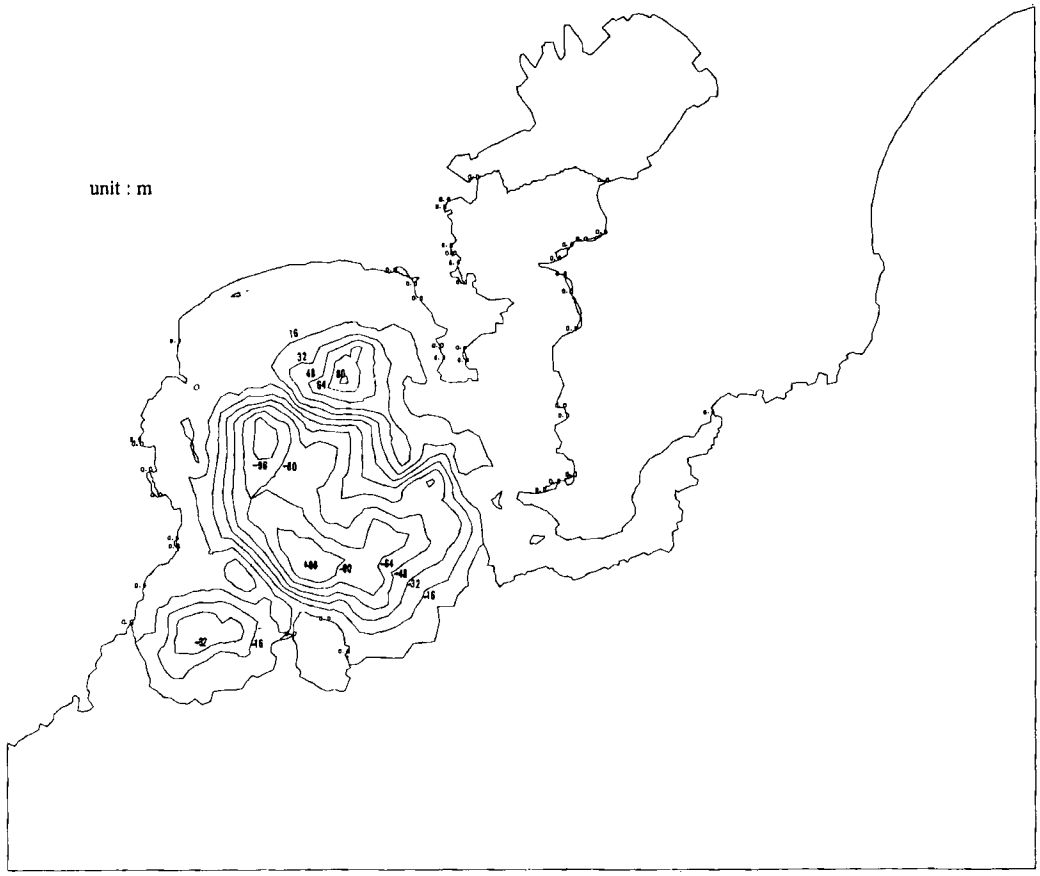

Figure 24. Distribution of bottom deformation

CONCLUSIONS

An automatic mesh generation method for the finite element analysis of shallow water flow has been presented in this paper. In order to show the efficiency of this method, it has been applied to some shallow water problems. The numerical solutions obtained have been compared with the analytical and observed ones. The conclusions derived are as follows.

1. The finite element mesh can be generated so that the element Courant number is nearly constant in the whole domain with complex geometry. It follows that the numerical accuracy improves automatically. Moreover, since it is possible to take larger values of the time increment, the computational time can be reduced using the present mesh.
2. The finite element mesh data, including the data of water depth, can be prepared automatically. Thus the effort necessary to prepare the mesh data can be greatly reduced.
3. It is possible to control the total numbers of elements and nodes by choosing the appropriate input data for the time increment Δt and node interval δ.

From the results obtained in this paper it can be concluded that the present method provides a useful and powerful tool for the preparation of finite element mesh data for shallow water analysis.

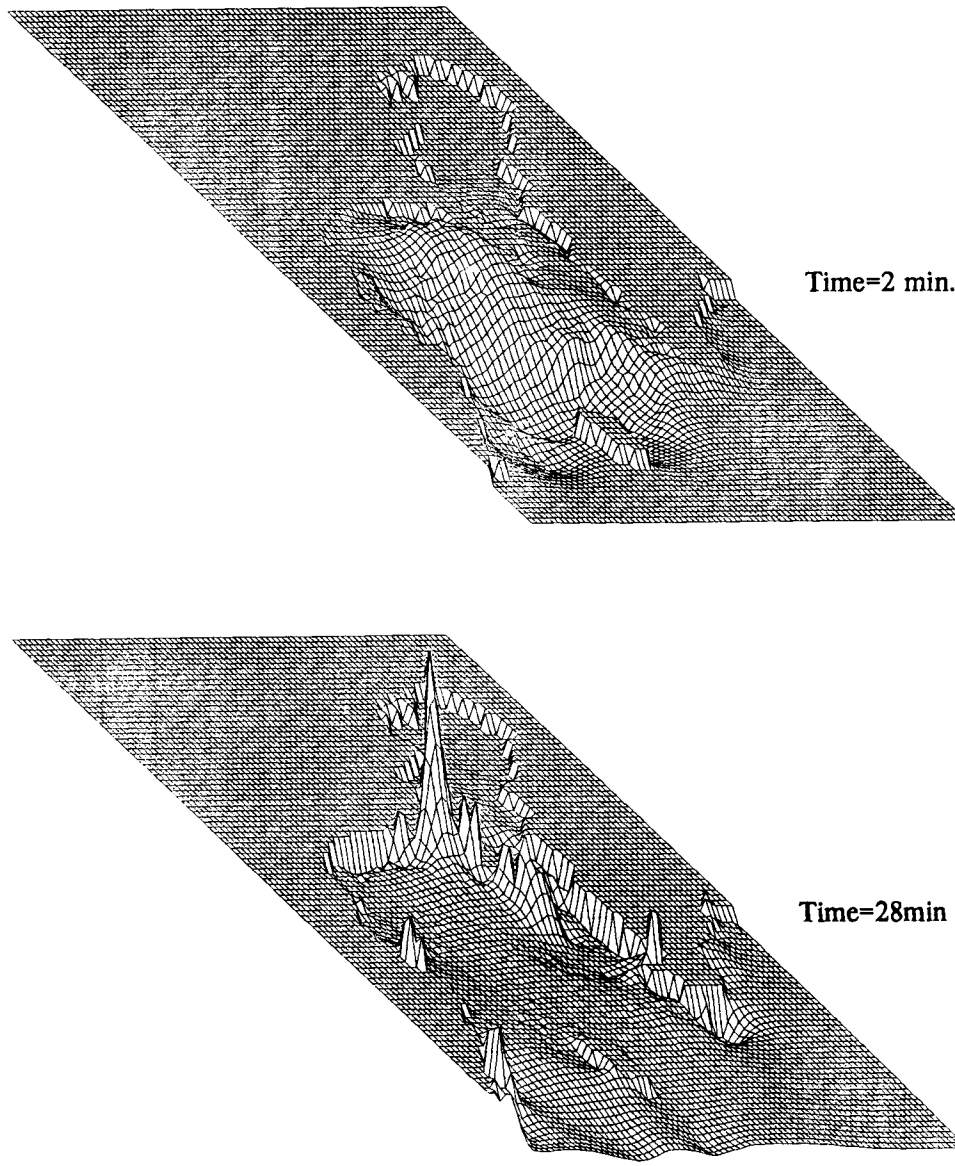

Figure 25. Computed tsunami wave propagation

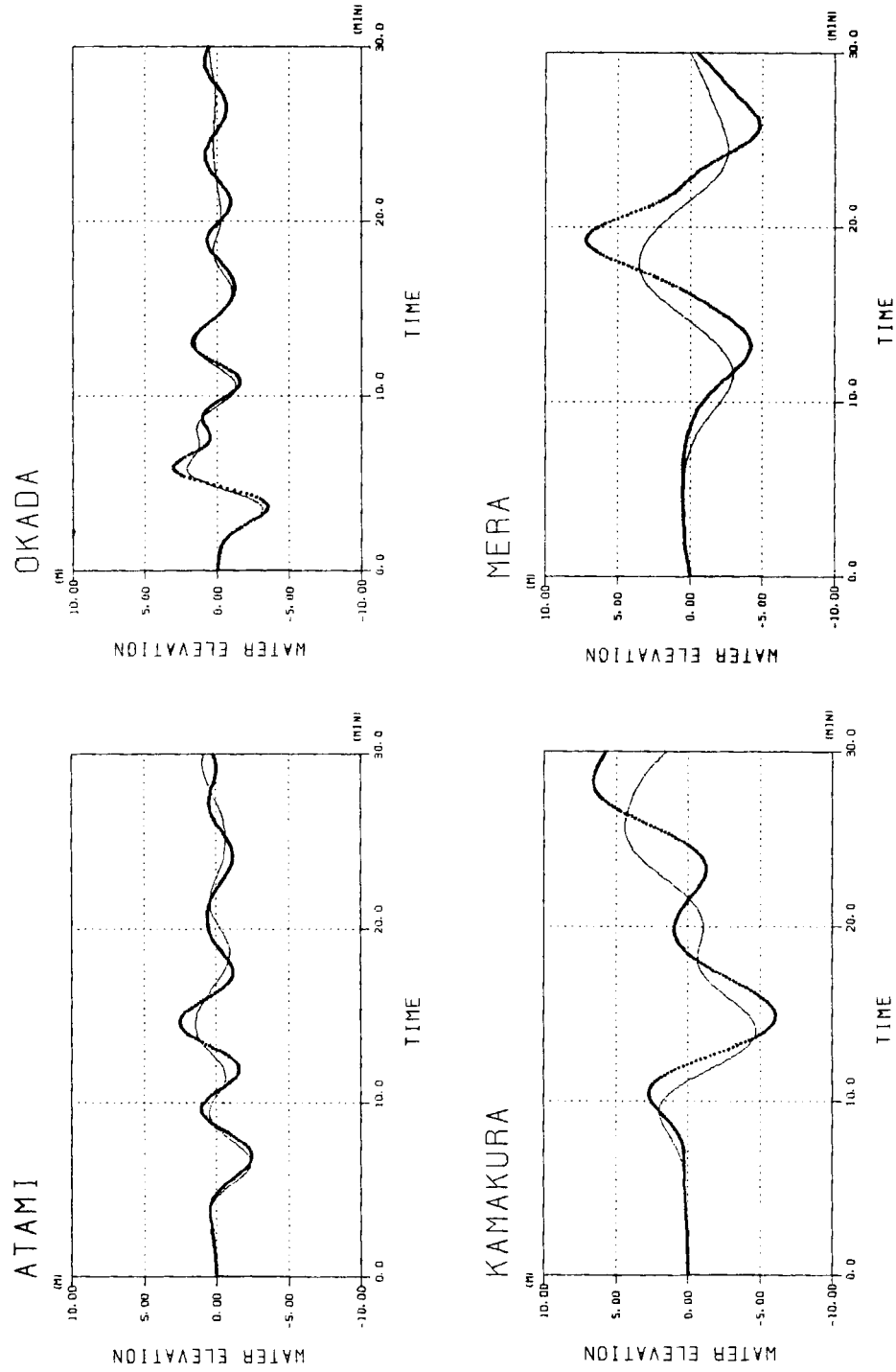

Figure 26. Time history of water elevation

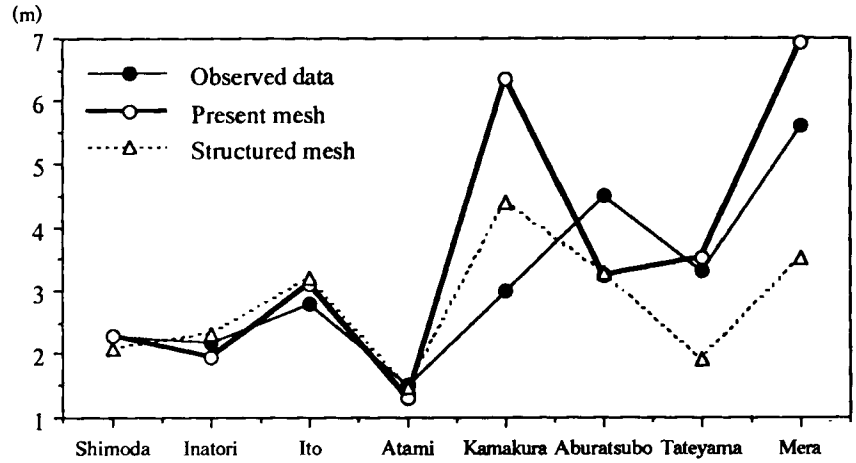

Figure 27. Comparison of maximum water elevation

ACKNOWLEDGEMENTS

The authors wish to express their gratitude to professor Mutsuto Kawahara and Mr. Toshio Kodama of Chuo University for their useful suggestions, and to Mr. Takeshi Imai and Mr. Hiroaki Yamada, students of Chuo University, for their help in performing computer runs.

REFERENCES

1. H. Kardestuncer (ed.), *Finite Element Handbook*, McGraw-Hill, London, 1987, pp. 3.81–3.101.
2. C. C. Mei, *The Applied Dynamics of Ocean Surface Waves*, Wiley, New York, 1983.
3. W. C. Thacker, A Gonzales and G. E. Putland, 'A method for automating the construction of irregular computational grids for storm surges forecast models', *J. Comput. Phys.*, **37**, 371–387 (1980).
4. I. J. Westwood and K.-P. Holtz, 'Automatic optimization of irregular meshes for natural flow computation', *Proc. Int. Conf. on Hydrosoft 86*, Springer, Berlin, 1986, pp. 423–425.
5. P. Nielsen and O. Skovgaard, 'A scheme for automatic generation of boundary-fitted depth- and depth-gradient-dependent grids in arbitrary two-dimensional regions, *Int. j. numer. methods fluids*, **10**, 741–752 (1990).
6. P. Nielsen and O. Skovgaard, 'The effect of using non-orthogonal boundary-fitted grids for solving the shallow water equations', *Int. j. numer. methods fluids*, **11**, 117–188 (1991).
7. J. C. Cavendish, D. A. Field and W. H. Wung, 'An approach to automatic three-dimensional finite element mesh generation, *Int. j. numer. methods eng.*, **21**, 329–348 (1985).
8. S. H. Lo, 'A new mesh generation scheme for arbitrary planner domains', *Int. j. numer. methods eng.*, **21**, 1403–1426 (1985).
9. K. Kashiyama and M. Kawahara, 'Interpolation method for preparation of input data of water depth in finite element analysis of shallow water flow', *Eng. Comput.*, **2**, 266–270 (1985).
10. N. Kikuchi, 'Adaptive grid-design methods for finite element analysis', *Comput. Methods Appl. Mech. Eng.*, **55**, 129–160 (1986).
11. A. Wilslow, 'Numerical solution of the quasilinear Poisson equation', *J. Comput. Phys.*, **1**, 149–172 (1966).
12. M. Kawahara, H. Hirano, K. Tsubota and K. Inagaki, 'Selective lumping finite element method for shallow water flow', *Int. j. numer. methods fluids*, **2**, 89–112 (1982).
13. M. Kawahara and K. Kashiyama, 'Selective lumping finite element method for nearshore current', *Int. j. numer. methods fluids*, **4**, 71–97 (1984).
14. K. Kajiura, 'Local behavior of tsunami', in D. G. Provis and R. Radok (eds), *Waves on Water of Variable Depth, Lecture Notes in Physics*, Vol. **64**, Springer, Berlin, 1977, pp. 72–79.
15. I. Aida, 'A numerical experiment for the Tsunami accompanying the Kanto earthquake of 1923', *Bull. Earthq. Res. Inst., Univ. Tokyo*, **48**, 73–86 (1970) (in Japanese).
16. M. Kawahara, T. Kodama and M. Kinoshita, 'Finite element method for tsunami wave propagation analysis considering the open boundary conition', *Comput. Math. Appl.*, **16**, 139–152 (1988).